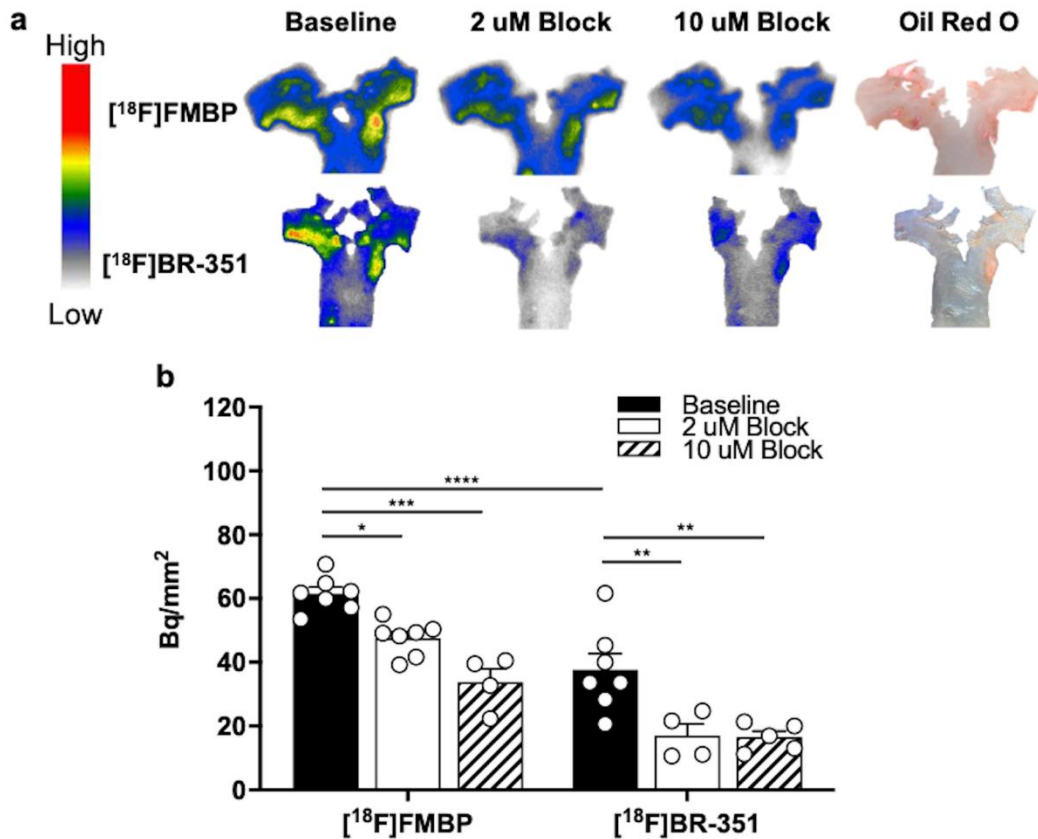
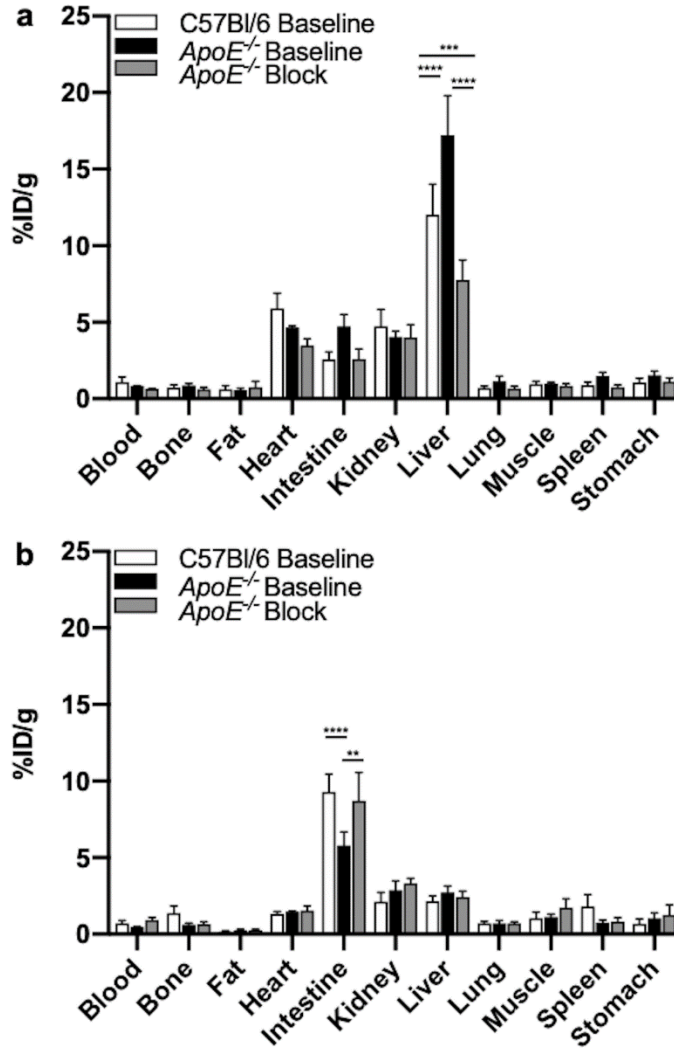


**Figure 1.** Structure of target radiotracers. **(a)** [<sup>18</sup>F]FMBP **(b)** [<sup>18</sup>F]BR-351.



**Figure 2.** *In vitro* target specificity and co-localization with lipid content in atherosclerotic aortae. **(a)** Representative *ApoE*<sup>-/-</sup> aortic *en face in vitro* autoradiographs 1 h after incubation with 45 kBq [<sup>18</sup>F]FMBP or [<sup>18</sup>F]BR-351. Homologous blocking was performed by co-incubation of 2 μM and 10 μM non-radioactive FMBP or BR-351. Corresponding bright-field images of ORO stains are shown. Note the slight fold in the [<sup>18</sup>F]BR-351 aorta under 10 μM blocking conditions. **(b)** [<sup>18</sup>F]FMBP and [<sup>18</sup>F]BR-351 aortic lesion uptake. Two-way ANOVA: \*\*\*\**P* < 0.0001, \*\*\**P* = 0.0001, \*\**P* < 0.0046, \* *P* = 0.0363, *n* = 4–7 per group.



**Figure 3.** *Ex vivo* biodistributions 30 min after intravenous radiotracer administration (15 MBq) via the lateral tail vein. **(a)** [<sup>18</sup>F]FMBP. Two-way ANOVA: \*\*\*\* $P < 0.0001$ , \*\*\* $P = 0.0007$ . **(b)** [<sup>18</sup>F]BR-351. Two-way ANOVA: \*\*\*\* $P < 0.0001$ , \*\* $P = 0.0011$ ,  $n = 6-7$  per group ( $n = 2-3$  for blood, heart, and muscle).



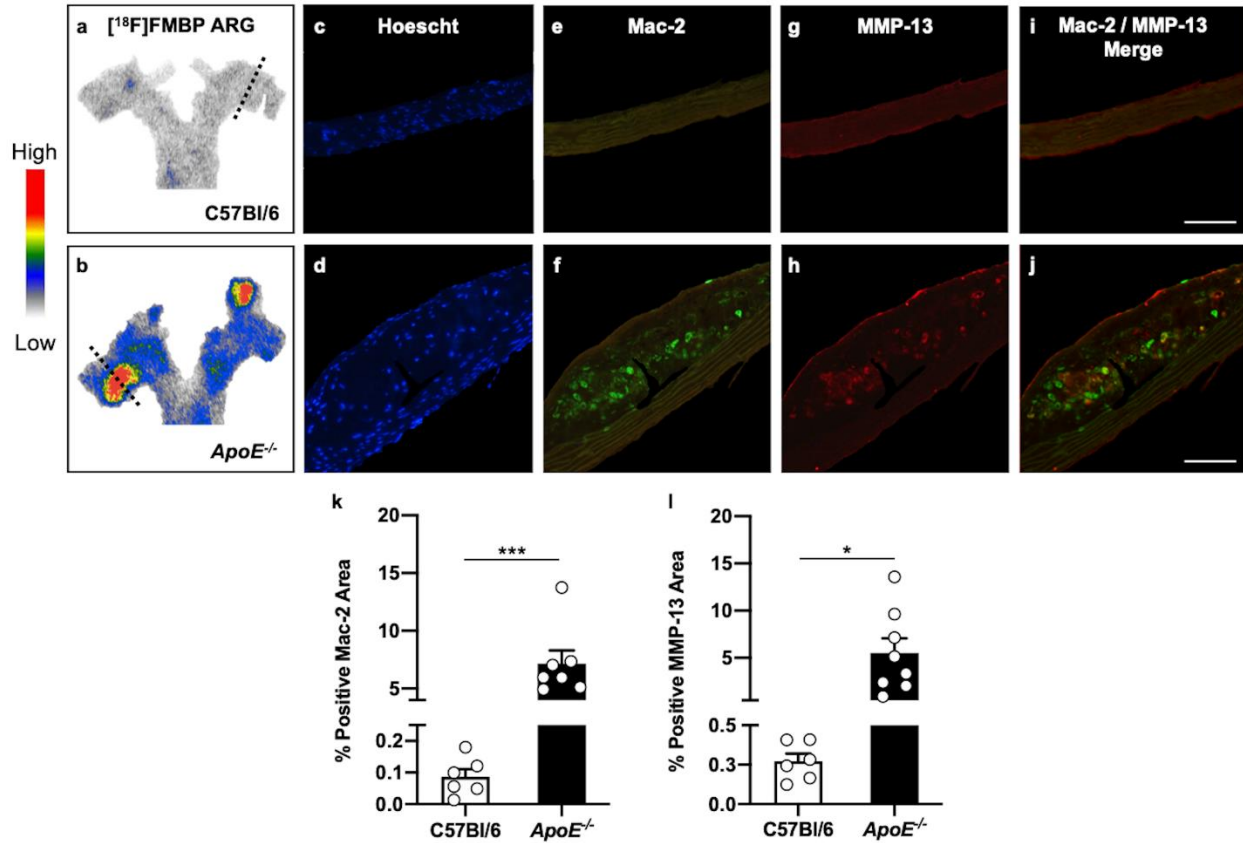


**Figure 5.** Immunofluorescent staining of atherosclerotic lesions detected by  $[^{18}\text{F}]$ FMBP *ex vivo* autoradiography. **(a/b)** Selected  $[^{18}\text{F}]$ FMBP *ex vivo* autoradiographs in C57Bl/6 and  $ApoE^{-/-}$  mice. Corresponding composite images of cross-sections following immunofluorescent staining for **(c/d)** Hoescht, **(e/f)** Mac-2, and **(g/h)** MMP-13. **(i/j)** Mac-2 and MMP-13 merge. Scale bar = 100  $\mu\text{m}$ . **(k/l)** Quantification of percentage positive Mac-2 and MMP-13 areas in  $ApoE^{-/-}$  and C57Bl/6 mice. Unpaired t-test: \*\*\* $P = 0.0001$ , \* $P = 0.0127$ ,  $n = 6-8$  per group.